Phys Chem Minerals (2017) 44:163–170
DOI 10.1007/s00269-016-0845-2

ORIGINAL PAPER

Raman spectroscopic study of $MnAl_2O_4$ galaxite at various pressures and temperatures

Shuangmeng Zhai[1] · Yuan Yin[1,2] · Sean R. Shieh[3] · Yun-Yuan Chang[4] · Tianqi Xie[3] · Weihong Xue[1]

Received: 2 May 2016 / Accepted: 22 September 2016 / Published online: 1 October 2016

Abstract The vibrational properties of synthetic galaxite, $MnAl_2O_4$, were investigated at various pressures (0–29.7 GPa) and temperatures (80–973 K), respectively. The Raman frequencies of all observed bands for galaxite continuously increase with increasing pressure and decrease with increasing temperature, respectively. The quantitative analysis shows that the lowest frequency T_{2g} mode has the smallest isothermal mode Grüneisen parameter. Combined with previous studies, the thermal Grüneisen parameter of galaxite is determined to be 1.23(5). The quantitative analysis of temperature dependences of Raman bands yields that the lowest frequency T_{2g} mode has the largest isobaric mode Grüneisen parameter. The intrinsic anharmonic mode parameters are also calculated and nonzero, indicating an existence of intrinsic anharmonicity for $MnAl_2O_4$ spinel.

Keywords Galaxite · $MnAl_2O_4$ · Raman spectra · High pressure · Various temperature

✉ Shuangmeng Zhai
zhaishuangmeng@vip.gyig.ac.cn

[1] Key Laboratory of High-Temperature and High-Pressure Study of the Earth's Interior, Institute of Geochemistry, Chinese Academy of Sciences, Guiyang 550081, China

[2] College of Earth Science, University of Chinese Academy of Sciences, Beijing 100049, China

[3] Department of Earth Sciences, University of Western Ontario, London, ON N6A 5B7, Canada

[4] Institute of Earth Sciences, Academia Sinica, Taipei 115, Taiwan

Introduction

Compounds with spinel-type structure occupy an outstanding position in geology (Biagioni and Pasero 2014). Minerals with spinel structure have a great relevance in geosciences since they are important main or accessory components in different rocks in the Earth's crust and upper mantle. The physical properties and stabilities of many spinels under high pressures and/or temperatures had been intensively investigated in past decades. However, there are still several open issues remained to be resolved.

Galaxite, $MnAl_2O_4$, an important Mn-rich mineral first described by Ross and Kerr (1932) from a vein containing unusual Mn minerals equilibrated under amphibolites facies conditions, was widely found in metamorphosed rocks (Essene and Peacor 1983; Flohr and Huebner 1992; Gnos and Peters 1995; Lucchesi et al. 1997; Beard and Tracy 2002; Brugger and Meisser 2006). Galaxite exhibits a normal spinel structure as reported by Essene and Peacor (1983), Lucchesi et al. (1997) and Hålenius et al. (2007, 2011). Optical absorption spectroscopic data of synthetic $MnAl_2O_4$ were also reported in previous studies (Hålenius et al. 2007, 2011; Nyquist and Hålenius 2014). Recently, the elastic constants C_{ij} of synthetic single crystal $MnAl_2O_4$ were investigated by using Brillouin spectroscopy at ambient conditions (Bruschini et al. 2015). However, little information about the vibrational behavior of the galaxite $MnAl_2O_4$ under high pressures and temperatures is available.

On the other hand, the quasi-harmonic approximation usually plays an important role in thermodynamic modeling and theory of equations of state of minerals. In this approximation, thermodynamic properties are calculated from the vibrational spectrum, which is assumed to depend only on volume and not on temperature. However,

the intrinsic anharmonic effects, ignored in this approximation and leading to the temperature dependence of phonon frequencies, become important at high temperatures (especially at low pressures) (Oganov and Dorogokupets 2004). In fact, the intrinsic anharmonicity can be estimated from the vibrational spectroscopic information of minerals (Gillet et al. 1989). Yet, there is no information about the intrinsic anharmonicity of $MnAl_2O_4$ galaxite.

In this paper, we report the micro-Raman spectroscopic measurements on the galaxite up to about 30 GPa at room temperature and in the temperature range of 80–973 K at ambient pressure, respectively. The effects of pressure and temperature on the characteristic Raman active modes of galaxite were analyzed. Based on the obtained results and combined with previous studies, the isothermal and isobaric mode Grüneisen parameters of $MnAl_2O_4$ spinel were calculated, and the intrinsic anharmonicity was estimated.

Experimental

The high-purity galaxite $MnAl_2O_4$ sample was prepared by a solid-state reaction. Reagent-grade MnO and Al_2O_3 powders were mixed in the proportion corresponding to the $MnAl_2O_4$ stoichiometry, and the mixture was ground sufficiently and then pressed into pellets with a diameter of 5 mm. The pellets were sintered at 1773 K for 24 h in an argon atmosphere. The synthesized product was ground finely and characterized by powder X-ray diffraction. The powder X-ray diffraction pattern confirms that the synthetic product is pure $MnAl_2O_4$ spinel phase. The Rietveld refinement of the powder X-ray pattern yields a unit cell parameter of 8.2272(2) Å for the synthesized $MnAl_2O_4$ spinel, which is consistent with previous studies (Hill et al. 1979; Siddiqi et al. 1987; Tristan et al. 2005; Edrissi et al. 2012).

High-pressure Raman measurements were taken using a symmetric type of diamond anvil cell with a pair of 500-μm culet diamond anvils. The experimental method used in this study was similar to previous studies (Zhai et al. 2015, 2016). A stainless steel plate with an initial thickness of 250 μm was used as gasket. The central area of the gasket was pre-indented to a thickness of about 30 μm, and a hole of 100 μm in diameter was drilled at the center. The synthetic sample was loaded into the sample chamber with Ar as the pressure medium. Ruby (Cr^{3+} doped α-Al_2O_3) spheres as pressure marker were carefully placed inside the same chamber. The pressures were determined by the ruby fluorescence method (Mao et al. 1978). Micro-Raman spectra were collected using a custom-built Raman system at the University of Western Ontario. An argon-ion laser with a wavelength of 514.5 nm was used as exciting source, and a spectrometer with a liquid nitrogen cooled CCD detector was used to collect the Raman data. The spectrometer was calibrated using a neon lamp, and the precision of the frequency determination was about 1 cm^{-1}. The data collection time was 120 s for each spectrum.

A small piece of $MnAl_2O_4$ spinel sample was prepared for Raman spectroscopic measurements at various temperatures. The method and procedure in various temperature experiments were similar to previous studies (Zhai et al. 2011, 2014). A sintered polycrystalline sample of about 100 × 80 × 50 μm in size was put on a silica or sapphire window for low-temperature or high-temperature measurements, respectively. The silica window was placed at the center of a small silver block for freezing runs using THMSG 600, while the sapphire window was put into an alumina chamber in a Linkam TS 1500 for heating. Low temperatures are obtained by pumping liquid nitrogen through an annulus in the silver block, and a resistance heater opposes the cooling effect of the nitrogen to yield the desired temperature. In the heating mode, only the resistance heater was used along with a water cooling system and an S-type thermocouple was used. In both modes, the temperature control unit is completely automatic and can be programmed to maintain any desired temperature or to change temperature at a constant rate of 10 °C/min. The system has been calibrated at both high and low temperatures by observing phase changes in synthetic fluid inclusions placed in the center of the crucible. Horizontal thermal gradients may lead to errors of up to 1 % in temperature measurements. At each temperature step, the samples were kept at the new temperature for at least 10 min in cooling measurements and 5 min in heating measurements before recording the Raman spectra in order to allow the samples to reach thermal equilibrium. The Raman spectra of $MnAl_2O_4$ spinel at ambient pressure and various temperatures were recorded by a LabRam HR (Jobin–Yvon) spectrometer equipped with a holographic notch filter, 600 g/mm grating. The grating was kept stationary, while the temperature was varied to provide the most accurate means for directly comparing the variation of vibrational frequencies with temperature. The Raman shift is accurate to ±1 cm^{-1}, as determined by plasma and neon emission lines. The sample was illuminated with 514.5-nm laser excitation from a Spectra Physics model 2017 argon-ion laser, using a power of 3.4 mW at the samples. An SLM Plan 20× Olympus microscope objective was used to focus the laser beam and collect the scattered light. The focused laser spot on the sample was estimated to be 2–4 μm in diameter. The accumulation time for each spectrum was 30–90 s, and the final spectrum was the average of three collections.

The Raman shift of each band was obtained by Lorentzian curve fitting to get a reasonable approximation by using PeakFit program (SPSS Inc., Chicago).

Results and discussion

Galaxite is in a cubic structure with space group of *Fd-3 m* and $Z = 8$. According to the factor group analysis (White and DeAngelis 1967), the Raman active vibrations of cubic spinel are as following:

$$\Gamma = A_{1g} + E_g + 3T_{2g}$$

where E_g and T_{2g} modes are doubly and triply degenerate, respectively. Therefore, only five Raman active modes exist in normal non-defective spinels. However, non-stoichiometry, the presence of vacancies, interstitial cations and defects may result in activation of Raman modes not predicted by group theory (Errandonea 2014).

The Raman spectrum of $MnAl_2O_4$ at ambient conditions is shown in Fig. 1. Six bands were observed, including 201, 514 and 628 cm^{-1} for T_{2g} mode, 396 cm^{-1} for E_g mode, 696 and 752 cm^{-1} for A_{1g} mode, which are consistent with recent results (D'Ippolito et al. 2015). It is noticeable that the splitting of the high-frequency A_{1g} mode is similar to that observed in $CoFe_2O_4$, and could be due to a partial cation distribution (Chandramohan et al. 2011). Although the investigated galaxite $MnAl_2O_4$ has a normal spinel structure, it shows some degree of inversion. Indeed, the minor disordered cation distribution in $MnAl_2O_4$ was observed in natural and synthetic galaxite samples (Greenwald et al. 1954; Essene and Peacor 1983; Lucchesi et al. 1997; Hålenius et al. 2007, 2011). Consequently, the disordering within the crystal structure of $MnAl_2O_4$ causes the appearance of an additional Raman active peak at 696 cm^{-1}.

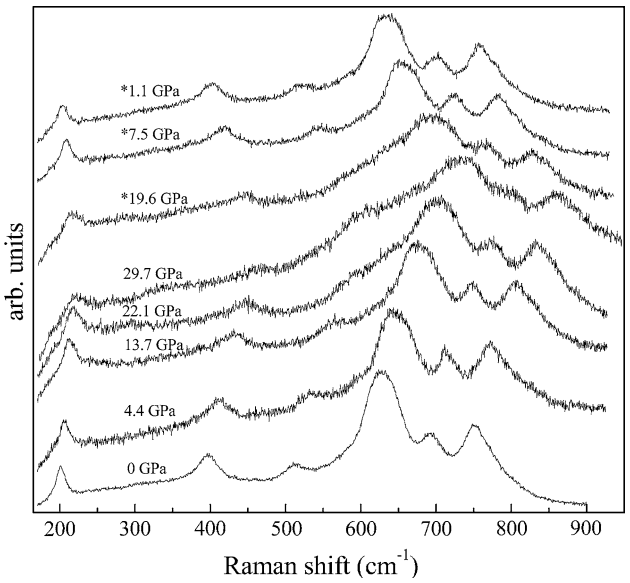

Fig. 1 Typical Raman spectra of galaxite $MnAl_2O_4$ at high pressures and room temperature. The pressure values with *asterisk symbols* represent the Raman spectra collected during decompression

Pressure dependence of Raman spectra

High-pressure Raman spectra of galaxite $MnAl_2O_4$ were collected up to 29.7 GPa, and some spectra were collected during decompression. The typical Raman spectra of $MnAl_2O_4$ at high pressures are also reproduced in Fig. 1. It is obvious that, with pressure increasing, the Raman peaks of $MnAl_2O_4$ gradually shift to higher frequencies and become weaker. This is reasonable since the Al–O and Mn–O bond lengths become shorter with increasing pressure and shorter bond lengths imply stronger bonds, i.e., larger force constants, and consequently higher vibrational frequencies according to Szigeti relationship described classically by a harmonically oscillating ball and spring model (Parker and Seddon 1992). During compression, there are almost no changes in the Raman features of $MnAl_2O_4$. It seems that the relative intensity of the two A_{1g} modes does not change during compression, indicating that the cation disorder in $MnAl_2O_4$ spinel remains stable during compression, which is somehow different from that of $CoFe_2O_4$. The cation inversion in $CoFe_2O_4$ was unchanged under quasi-hydrostatic conditions but enhanced by pressure under no hydrostatic conditions (Saccone et al. 2015). Moreover, the Raman peaks considerably broaden and loss intensity at 29.7 GPa, which is probably not due to the non-hydrostaticity though Ar was used as pressure medium. It could be related to a distortion of the cubic spinel structure to the tetragonal under compression, as found in $ZnGa_2O_4$ spinel at a similar pressure (31 GPa) (Errandonea et al. 2009). Further study is required to confirm the possible structure change in $MnAl_2O_4$ spinel under high-pressure conditions.

The Raman shift versus pressure plot of $MnAl_2O_4$ is illustrated in Fig. 2. The Raman shifts of modes in $MnAl_2O_4$ change continuously with pressure, and the slopes are various for different modes. In this study, argon was used as pressure medium, which gives a hydrostatic limit of about 10 GPa (Klotz et al. 2009). Therefore, in order to avoid the effect of non-hydrostatic compression, the pressure coefficients ($\partial\nu_i/\partial P$) of different Raman vibrations of $MnAl_2O_4$ spinel were determined using the data below 10 GPa. As listed in Table 1, the pressure coefficients ($\partial\nu_i/\partial P$) of active Raman vibrations in $MnAl_2O_4$ vary from 0.88(4) to 4.61(16) cm^{-1}/GPa.

The pressure coefficients of the different Raman modes can be used to obtain the isothermal mode Grüneisen parameters, which can be calculated by the following equation (Gillet et al. 1989; Okada et al. 2008):

$$\gamma_{iT} = K_T(\partial \ln \nu_i/\partial P)_T$$

where ν_i is the Raman shift of the i-th vibrational mode, K_T is the isothermal bulk modulus. There is no available data about K_T of $MnAl_2O_4$ spinel. However, the adiabatic bulk modulus K_S of $MnAl_2O_4$ spinel was obtained as 200 GPa by Brillouin spectroscopy at ambient conditions (Bruschini et al. 2015). Actually the difference between K_T and K_S is usually in the order of 1–2 % for the most common oxide and silicate minerals (Bruschini et al. 2015). Therefore, the isothermal bulk modulus K_T of $MnAl_2O_4$ spinel can be estimated as 198 GPa, which was used to calculate the isothermal mode Grüneisen parameters as shown in Table 1. The resulting isothermal mode Grüneisen parameters of $MnAl_2O_4$ spinel are from 0.86(4) to 1.77(6), which is comparable to previous studies of other spinels. In previous experimental or theoretical studies, the isothermal mode Grüneisen parameters of some other spinels were reported, including $MgAl_2O_4$ (0.64–2.0, Chopelas and Hofmeister 1991), $ZnCr_2O_4$ (1.14–2.08, Wang et al. 2002a), Zn_2TiO_4 (0.63–1.02, Wang et al. 2002b), $ZnFe_2O_4$ (0.52–1.88, Wang et al. 2003), $ZnAl_2O_4$ (0.9–1.5, López-Moreno et al. 2011), $ZnGa_2O_4$ (1.0–1.8, López-Moreno et al. 2011), $MgCr_2O_4$ (1.27–2.03, Yong et al. 2012), $CoCo_2O_4$ (0.57–1.32, Bai et al. 2012). The lowest frequency T_{2g} mode has the smallest isothermal mode Grüneisen parameter, indicating a smallest pressure effect. In previous study, the lowest frequency T_{2g} mode is associated with a complete translation of the MnO_4 within the $MnAl_2O_4$ spinel structure (D'Ippolito et al. 2015). However, in the structure of $MnAl_2O_4$, the AlO_6 octahedron shares oxygens with neighbor MnO_4 tetrahedra (Hålenius et al. 2011), which means that both the MnO_4 tetrahedra and AlO_6 octahedra translate if the T_{2g} mode at ~200 cm^{-1} contains translations of oxygens. Therefore, the lowest frequency T_{2g} mode cannot be assigned to only translation of MnO_4 or AlO_6. In other words, the T_{2g} mode at ~200 cm^{-1} may be a combination associated with both MnO_4 and AlO_6. The two A_{1g} modes show similar Grüneisen parameters, as listed in Table 1, which indicates that the pressure effect on the two A_{1g} modes is similar during compression. The A_{1g} mode is assigned to the Al–O stretching vibration of AlO_6 groups (D'Ippolito et al. 2015).

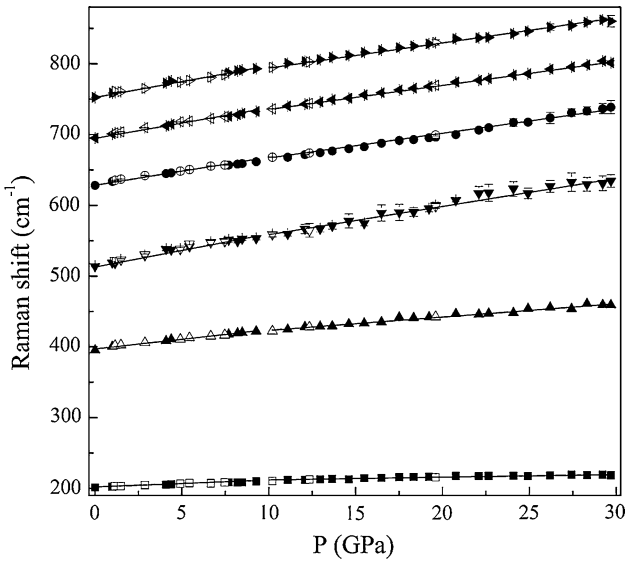

Fig. 2 Pressure dependence of the Raman bands of galaxite $MnAl_2O_4$ at room temperature. *Open symbols* represent the Raman shifts during decompression

The thermal Grüneisen parameter (γ_{th}) can be calculated by the weighted average of the mode Grüneisen parameters (γ_{iT}) determined experimentally, using the following equation (e.g., Chopelas 1996):

$$\gamma_{th} = \frac{\sum_i C_{\nu_i}\gamma_{iT}}{\sum_i C_{\nu_i}}$$

where C_{ν_i} is a harmonic heat capacity contribution of the i-th vibrational mode. The C_{ν_i} values can be estimated from the Einstein function:

$$C_{\nu_i} = k\left(\frac{h\nu_i}{kT}\right)^2 \exp\left(\frac{h\nu_i}{kT}\right) \Big/ \left[\exp\left(\frac{h\nu_i}{kT}\right) - 1\right]^2$$

Table 1 Constants determined in the expression: $\nu_P = \nu_{i0} + (\partial\nu_i/\partial P) \times P$, $\nu_T = \nu_{i0} + (\partial\nu_i/\partial T) \times (T - 300)$, the isothermal ($\gamma_{iT}$) and isobaric ($\gamma_{iP}$) mode Grüneisen parameters, and the intrinsic anharmonic mode parameter (α_i) for $MnAl_2O_4$ spinel

Modes	ν_0	$\partial\nu_i/\partial P$	R_1^2	γ_{iT}	$(\partial\nu_i/\partial T) \times 10^2$	R_2^2	γ_{iP}	$\alpha_i \times 10^5$
T_{2g}	201	0.88(4)	0.971	0.86(4)	−1.20(5)	0.888	3.17(14)	−4.28(27)
E_g	396	2.83(10)	0.982	1.41(5)	−2.14(9)	0.865	2.90(12)	−2.76(24)
T_{2g}	514	4.61(16)	0.984	1.77(6)	−2.63(8)	0.848	2.71(9)	−1.74(20)
T_{2g}	628	3.72(12)	0.992	1.17(5)	−1.82(6)	0.937	1.54(6)	−0.69(14)
A_{1g*}	696	3.90(10)	0.986	1.11(3)	−1.91(8)	0.875	1.47(6)	−0.67(12)
A_{1g}	752	4.39(10)	0.992	1.15(3)	−2.17(5)	0.933	1.54(3)	−0.73(8)

ν_P and ν_T are in cm^{-1}, $\partial\nu_i/\partial P$ is in cm^{-1} GPa^{-1}, $\partial\nu_i/\partial T$ is in cm^{-1} K^{-1}, ν_0 was observed frequency (in cm^{-1}) at ambient conditions. R_1^2 and R_2^2 are the correlation coefficients. The isothermal Grüneisen parameter γ_{iT} was calculated with isothermal bulk modulus of $K_T = 198$ GPa estimated in this study. The unit of α_i is K^{-1}

where v_i is the vibrational frequency of the i-th mode given in 1/s, T is the temperature in K, while k and h are the Boltzmann and Plank constants, respectively. In this study, we calculated C_{v_i} using v_0 observed at ambient conditions. The thermal Grüneisen parameter γ_{th} of $MnAl_2O_4$ was obtained as 1.23(5) using 6 γ_{iT} values listed in Table 1.

Temperature dependence of Raman spectra

The Raman spectra of $MnAl_2O_4$ spinel were collected in the temperature range from 80 to 973 K at ambient pressure. According to the phase diagram of MnO-Al_2O_3 system at ambient pressure (Jung et al. 2004), no phase transition is expected in this investigated temperature range. The lower temperature is limited by the liquid nitrogen used to cool the sample stage. Some typical Raman spectra of $MnAl_2O_4$ spinel at various temperatures are shown in Fig. 3. Generally, with increasing temperatures, the Raman bands of vibrational modes shift to lower frequency regions and become broader. This is reasonable since the bond length becomes longer, and longer bond length implies weaker bond, i.e., small force constant, and consequently lower vibrational frequencies according to Szigeti relationship (Parker and Seddon 1992). Due to the weakness and overlap, it is difficult to position the peaks in the Raman spectra collected at 773 K and higher temperatures. Therefore, the temperature dependence of the Raman active modes was determined using the spectra collected below 773 K.

The temperature variations of Raman frequencies for all measurable modes are illustrated in Fig. 4. Generally, the Raman frequencies for all bands of $MnAl_2O_4$ spinel decrease with increasing temperature in the investigated temperature range. For quantitative analysis, nonlinear temperature dependence for the frequency of any Raman band is possible (Lin et al. 2000; Liu et al. 2009). However, in the present study, linear fitting may be more suitable for all observed bands shown in Fig. 4. The constants derived by linear regressions of the vibrations are listed in Table 1. Contrasting to the pressure dependence, all bands of the $MnAl_2O_4$ spinel show negative temperature dependence. The temperature coefficients ($\partial v_i/\partial T$) of vibrations in $MnAl_2O_4$ vary from $-2.63(8)$ to $-1.20(5) \times 10^{-2}$ cm^{-1}/K.

The temperature coefficients of the different Raman modes can be adopted to calculate the isobaric mode Grüneisen parameters, γ_{iP}, defined as the following expression (Gillet et al. 1989; Okada et al. 2008):

$$\gamma_{iP} = -1/\alpha(\partial \ln v_i/\partial T)_P$$

where v_i is the vibrational frequency of the i-th band and α is the thermal expansivity. No thermal expansion coefficient α for $MnAl_2O_4$ spinel is reported. But it can be derived from other available parameters since the thermal Grüneisen parameter can be expressed as:

$$\gamma_{th} = \alpha K_S V/C_P$$

where α, K_S, V and C_P are thermal expansion coefficient, adiabatic bulk modulus, molar volume and heat capacity, respectively. Using previously reported adiabatic bulk modulus K_S of 200 GPa (Bruschini et al. 2015), unit cell edge of

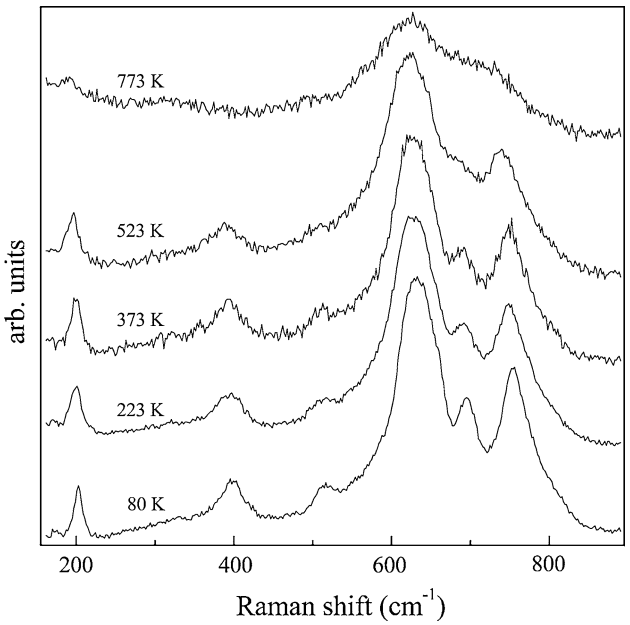

Fig. 3 Typical Raman spectra of galaxite $MnAl_2O_4$ at various temperatures and ambient pressure

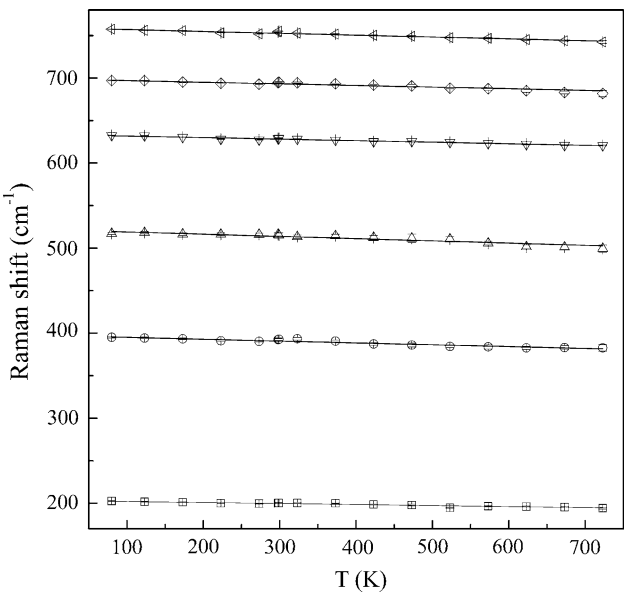

Fig. 4 Temperature dependence of the Raman bands of galaxite $MnAl_2O_4$ at ambient pressure

8.2272 Å (this study), heat capacity C_P of 126.26 J/mol/K (Navarro et al. 2012) and thermal Grüneisen parameter γ_{th} of 1.23 (this study) at room temperature, the thermal expansion coefficient can be calculated as 1.85×10^{-5} K^{-1} at room temperature. The isobaric mode Grüneisen parameters γ_{iP} then can be calculated, as listed in Table 1. The resulting isobaric mode Grüneisen parameters of $MnAl_2O_4$ spinel range from 1.47(6) to 3.17(14). It seems that the low-frequency modes show larger isobaric mode Grüneisen parameters than those of the high-frequency modes, which indicates a decreasing relative effect of temperature on the vibrational frequency of Raman modes. The lowest frequency T_{2g} mode has a largest isobaric mode Grüneisen parameter, indicating the most sensitive to temperature. It may be associated with the polyhedral evolution in $MnAl_2O_4$ spinel under high temperatures. But currently no crystal structural information is available under high temperatures for $MnAl_2O_4$ spinel.

For each mode of $MnAl_2O_4$ spinel, the isothermal mode Grüneisen parameter is smaller than the isobaric mode Grüneisen parameter. Therefore, an intrinsic anharmonicity exists, which plays an important role in equations of state of $MnAl_2O_4$ spinel intended for calculations of thermodynamic functions under conditions of the Earth's mantle. The intrinsic anharmonic mode parameter, α_i, can be determined according to the following definition (Mammone and Sharma 1979):

$$\alpha_i = \alpha(\gamma_{iT} - \gamma_{iP})$$

The values of calculated α_i for $MnAl_2O_4$ spinel are also listed in Table 1, which are nonzero and ranging from $-4.28(27) \times 10^{-5}$ K^{-1} to $-0.67(12) \times 10^{-5}$ K^{-1}. An average intrinsic anharmonic mode parameter of $-1.81(18) \times 10^{-5}$ K^{-1} can be obtained.

As pointed out by Gillet et al. (1989), the α_i parameter can be used to estimate the anharmonic contribution to the isochoric heat capacity according to following expression:

$$C_V = 3nR\sum_{i=1}^{m} C_{vi}(1 - 2\alpha_i T)$$

where n is the number of atoms in the mineral formula and R is the gas constant. By comparing above C_V with that obtained through Kieffer model (Kieffer 1979a, b), the anharmonic contribution can be estimated. The VDoS model for the Kieffer model calculation based on the acoustic velocities and the optic continuum. It should be mentioned that the number of formula per unit cell is not 8 but 2 because a reduced cell is used. So the total number of the vibrational modes is 42. Among them are three acoustic modes, and the rest are optic modes. Since acoustic velocities of $MnAl_2O_4$ spinel have not been measured, we first estimated compressional velocities (Vp) using Birch (1961) empirical

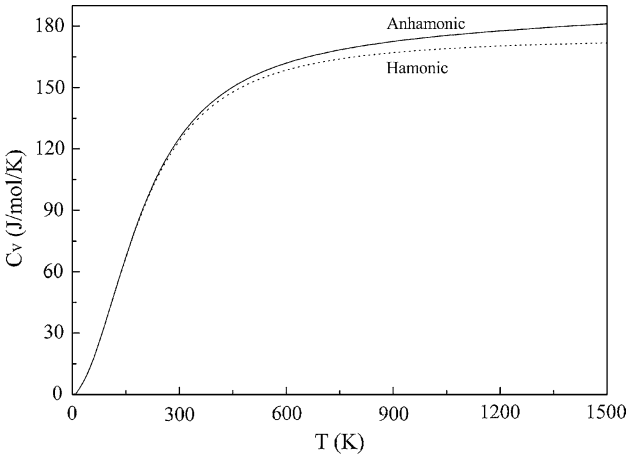

Fig. 5 Calculated harmonic and anharmonic isochoric heat capacity C_V

relationship Vp (km/s) $= -1.87 - 0.7 \times (m - 21) + 3.05$ ρ (g/cm^3), where ρ and m refer to density and mean atomic weight, respectively. Shear velocity (Vs) was estimated using the above Vp values and estimated bulk modulus (K_0). Directionally averaged acoustic velocities were obtained from the Vp and Vs values using the method by Kieffer (1979a). Infrared and Raman spectra are generally used for modeling of vibrational density of states for optic modes. In this study, we used the Raman spectrum of $MnAl_2O_4$ to constrain the distribution of the optic modes. We adopted an optic continuum model in the wave number range from 135 to 750 cm^{-1}. The isochoric heat capacity C_V was calculated based on the model of acoustic and optic mode mentioned above and shown as the dotted line in Fig. 5. The calculation using Kieffer model yields Debye temperature θ_D as 813.5 K and molar entropy S_{298} as 112 J/mol K, which are consistent with reported results of Navarro et al. (2012). Using an averaged α_i, the anharmonic isochoric heat capacity was calculated and illustrated as the solid line in Fig. 5. Based on the calculation, the anharmonic contribution becomes obvious with increasing temperature, e.g., about 4.9–6.0 % at 1500 K if the uncertainty of the averaged α_i is considered. Therefore, the harmonic or quasi-harmonic approximation is not suitable at high temperatures.

Acknowledgments The authors thank C. Lin for his help on various temperature Raman spectroscopic measurements, Dr. H. Kojitani for his help in calculation of Cv by using Kieffer model, and Prof. T. Tsuchiya for his editorial handling. Critical comments and suggestion from two anonymous reviewers are helpful to improve the manuscript. This work was financially supported by National Natural Science Foundation of China (Grants Nos 41372040 and U1532126), the Knowledge Innovation Program of the Institute of Geochemistry, Western Light Talents Training Program of Chinese Academy of Sciences, the Ministry of Science and Technology of Taiwan (Contracts Nos MOST 103-2811-M-001-182 and 104-2822-M-001-179) and the National Science and Engineering Research Council of Canada.

References

Bai L, Pravica M, Zhao Y, Park C, Meng Y, Sinogeikin SV, Shen G (2012) Charge transfer in spinel Co_3O_4 at high pressures. J Phys Condens Mater 24:435401

Beard JS, Tracy RJ (2002) Spinels and other oxides in Mn-rich rocks from the Hutter Mine, Pittsylvania County, Virginia, U.S.A.: implications for miscibility and solvus relations among jacobsite, galaxite, and magnetite. Am Mineral 87:690–698

Biagioni C, Pasero M (2014) The systematics of the spinel-type minerals: an overview. Am Mineral 99:1254–1264

Birch F (1961) The velocity of compressional waves in rocks to 10 kilobars, part 2. J Geophys Res 66:2199–2224

Brugger J, Meisser N (2006) Manganese-rich assemblages in the Barrhorn unit, Turtmanntal, central Alps, Switzerland. Can Mineral 44:229–248

Bruschini E, Speziale S, Andreozzi GB, Bosi F, Hålenius U (2015) The elasticity of $MgAl_2O_4$–$MnAl_2O_4$ spinels by Brillouin scattering and an empirical approach for bulk modulus prediction. Am Mineral 100:644–651

Chandramohan P, Srinivasan MP, Velmurugan S, Narasimhan SV (2011) Cation distribution and particle size effect on Raman spectrum of $CoFe_2O_4$. J Solid State Chem 184:89–96

Chopelas A (1996) Thermal expansivity of lower mantle phases MgO and $MgSiO_3$ perovskite at high pressure derived from vibrational spectroscopy. Phys Earth Planet Inter 98:3–15

Chopelas A, Hofmeister AM (1991) Vibrational spectroscopy of aluminate spinels at 1 atm and of $MgAl_2O_4$ to over 200 kbar. Phys Chem Miner 18:279–293

D'Ippolito V, Andreozzi GB, Bersani D, Lottici PP (2015) Raman fingerprint of chromate, aluminate and ferrite spinels. J Raman Spectrosc 46:1255–1264

Edrissi M, Soleymani M, Naderi M (2012) Synthesis of $MnAl_2O_4$ nanocrystallites by Pechini and sequential homogenous precipitation methods: characterization, product comparison, photocatalytic effect, and Taguchi optimization. J Sol-Gel Sci Technol 64:485–492

Errandonea D (2014) AB_2O_4 compounds at high pressure. In: Manjón FJ (ed) Pressure-induced phase transitions in AB_2X_4 chalcogenide compounds. Springer, Berlin, pp 53–73

Errandonea D, Kumar RS, Manjón FJ, Ursaki VV, Rusu EV (2009) Post-spinel transformations and equation of state in $ZnGa_2O_4$: determination at high pressure by in situ x-ray diffraction. Phys Rev B 79:024103

Essene EJ, Peacor DR (1983) Crystal chemistry and petrology of coexisting galaxite and jacobsite and other spinel solutions and solvi. Am Mineral 68:449–455

Flohr MJK, Huebner JS (1992) Mineralogy and geochemistry of two metamorphosed sedimentary manganese deposits, Sierra Nevada, California, USA. Lithos 29:57–85

Gillet P, Guyot F, Malezieux JM (1989) High-pressure, high-temperature Raman spectroscopy of Ca_2GeO_4 (olivine form): some insights on anharmonicity. Phys Earth Planet Inter 58:141–154

Gnos E, Peters T (1995) Tephroite-hausmannite-galaxite from a granulite-facies manganese rock of the United Arab Emirates. Contrib Mineral Petrol 120:372–377

Greenwald S, Pickart S, Grannis F (1954) Cation distribution and g factors of certain spinels containing Ni^{++}, Mn^{++}, Co^{++}, Al^{+++}, Ga^{+++}, and Fe^{+++}. J Chem Phys 22:1597–1600

Hålenius U, Bosi F, Skogby H (2007) Galaxite, $MnAl_2O_4$, a spectroscopic standard for tetrahedrally coordinated Mn^{2+} in oxygen-based mineral structures. Am Mineral 92:1225–1231

Hålenius U, Bosi F, Skogby H (2011) A first record of strong structural relaxation of TO_4 tetrahedra in a spinel solid solution. Am Mineral 96:617–622

Hill RJ, Craig JR, Gibbs GV (1979) Systematics of the spinel structure type. Phys Chem Miner 4:317–339

Jung I, Kang Y, Decterov SA, Pelton AD (2004) Thermodynamic evaluation and optimization of the MnO-Al_2O_3 and MnO-Al_2O_3-SiO_2 systems and applications to inclusion engineering. Metall Mater Trans B 35:259–268

Kieffer SW (1979a) Thermodynamics and lattice vibrations of minerals: 1. Mineral heat capacities and their relationships to simple lattice vibrational models. Rev Geophys 17:1–19

Kieffer SW (1979b) Thermodynamics and lattice vibrations of minerals: 3. Lattice dynamics and an approximation for minerals with application to simple substances and framework silicates. Rev Geophys 17:35–59

Klotz S, Chervin J, Munsch P, Le Marchand G (2009) Hydrostatic limits of 11 pressure transmitting media. J Phys D Appl Phys 42:075413

Lin CC, Liu LG, Mernagh TP, Irifune T (2000) Raman spectroscopic study of hydroxyl-clinohumite at various pressures and temperatures. Phys Chem Miner 27:320–331

Liu LG, Lin CC, Yung YJ, Mernagh TP, Irifune T (2009) Raman spectroscopic study of K-lingunite at various pressures and temperatures. Phys Chem Miner 36:143–149

López-Moreno S, Rodríguez-Hernández P, Muñoz A, Romero AH, Manjón FJ, Errandonea D, Rusu E, Ursaki VV (2011) Lattice dynamics of $ZnAl_2O_4$ and $ZnGa_2O_4$ under high pressure. Ann Phys 523:157–167

Lucchesi S, Russo U, Della Giusta A (1997) Crystal chemistry and cation distribution in some Mn-rich natural and synthetic spinels. Eur J Mineral 9:31–42

Mammone JF, Sharma SK (1979) Pressure and temperature dependence of the Raman spectra of rutile-structure oxides. Carnegie Institution Year Book, Washington, pp 369–373

Mao HK, Bell PM, Shaner JW, Steinberg DJ (1978) Specific volume measurements of Cu, Mo, Pd and Ag and calibration of the ruby R_1 fluorescence pressure gauge from 0.06 to 1 Mbar. J Appl Phys 49:3276–3283

Navarro RCS, Gomez AMS, de Avillez RR (2012) Heat capacity of stoichiometric Al_2MnO_4 spinel between 2 and 873 K. Calphad 37:11–17

Nyquist S, Hålenius U (2014) An EELS study of near edge structures of the oxygen K-edge in spinels. Phys Chem Miner 41:255–265

Oganov AR, Dorogokupets PI (2004) Intrinsic anharmonicity in equations of state and thermodynamics of solids. J Phys Condens Mater 16:1351–1360

Okada T, Narita T, Nagai T, Yamanaka T (2008) Comparative Raman spectroscopic study on ilmenite-type $MgSiO_3$ (akimotoite), $MgGeO_3$, and $MgTiO_3$ (geikielite) at high temperatures and high pressures. Am Mineral 93:39–47

Parker JM, Seddon AB (1992) Infrared-transmitting optical fibres. In: Cable M, Parker JM (eds) High-performance glass. Blackie, London, pp 252–286

Ross CS, Kerr PF (1932) The manganese minerals of a vein near Bald Knob, North Carolina. Am Mineral 17:1–18

Saccone FD, Ferrari S, Errandonea D, Grinblat F, Bilovol V, Agouram S (2015) Cobalt ferrite nanoparticles under high pressure. J Appl Phys 118:075903

Siddiqi SA, Akhtar P, Mateen A (1987) Structural characterization of hot-pressed manganese aluminium spinel. Mater Lett 5:475–478

Tristan N, Hemberger J, Krimmel A, Krug von Nidda H-A, Tsurkan V, Loidl A (2005) Geometric frustration in the cubic spinels MAl_2O_4 (M = Co, Fe, and Mn). Phys Rev B 72:174404

Wang Z, Lazor P, Saxena SK, Artioli G (2002a) High-pressure Raman spectroscopic study of spinel ($ZnCr_2O_4$). J Solid Sate Chem 165:165–170

Wang Z, Saxena SK, Zha CS (2002b) In situ X-ray diffraction and Raman spectroscopy of pressure-induced phase transformation in spinel Zn_2TiO_4. Phys Rev B 66:024103

Wang Z, Schiferl D, Zhao Y, O'Neill HSC (2003) High pressure Raman spectroscopy of spinel-type ferrite $ZnFe_2O_4$. J Phys Chem Solids 64:2517–2523

White WB, DeAngelis BA (1967) Interpretation of the vibrational spectra of spinels. Spectrochim Acta 23A:985–995

Yong W, Botis S, Shieh SR, Shi W, Withers AC (2012) Pressure-induced phase transition study of magnesiochromite ($MgCr_2O_4$) by Raman spectroscopy and X-ray diffraction. Phys Earth Planet Inter 196:75–82

Zhai S, Xue W, Lin C, Wu X, Ito E (2011) Raman spectra and X-ray diffraction of tuite at various temperatures. Phys Chem Miner 38:639–646

Zhai S, Lin C, Xue W (2014) Temperature-dependent Raman spectra of $Sr_3(PO_4)_2$ and $Ba_3(PO_4)_2$ orthophosphates. Vib Spectrosc 70:6–11

Zhai S, Shieh SR, Xue W, Xie T (2015) Raman spectra of stronadelphite $Sr_5(PO4)_3F$ at high pressures. Phys Chem Miner 42:357–361

Zhai S, Yin Y, Shieh SR, Shan S, Xue W, Wang C, Yang K, Higo Y (2016) High-pressure X-ray diffraction and Raman spectroscopy of $CaFe_2O_4$-type β-$CaCr_2O_4$. Phys Chem Miner 43:307–314